Environmental Science Processes & Impacts

PAPER

View Article Online
View Journal | View Issue

Cite this: *Environ. Sci.: Processes Impacts*, 2024, **26**, 2062

Differences in phytoplankton population vulnerability in response to chemical activity of mixtures†

Talles Bruno Oliveira dos Anjos, *[a] Quyen Nham, [b] Sebastian Abel, [a] Elin Lindehoff, [b] Clare Bradshaw [c] and Anna Sobek [a]

Hydrophobic organic contaminants (HOCs) affect phytoplankton at cellular to population levels, ultimately impacting communities and ecosystems. Baseline toxicants, such as some HOCs, predominantly partition to biological membranes and storage lipids. Predicting their toxic effects on phytoplankton populations therefore requires consideration beyond cell uptake and diffusion. Functional traits like lipid content and profile can offer insights into the diverse responses of phytoplankton populations exposed to HOCs. Our study investigated the vulnerability of five phytoplankton species populations to varying chemical activities of a mixture of polycyclic aromatic hydrocarbons (PAHs). Population vulnerability was assessed based on intrinsic sensitivities (toxicokinetic and toxicodynamic), and demography. Despite similar chemical activities in biota within the exposed algae, effects varied significantly. According to the chemical activity causing 50% of the growth inhibition (Ea_{50}), we found that the diatom *Phaeodactylum tricornutum* (Ea_{50} = 0.203) was the least affected by the chemical exposure and was also a species with low lipid content. In contrast, *Prymnesium parvum* (Ea_{50} = 0.072) and *Rhodomonas salina* (Ea_{50} = 0.08), both with high lipid content and high diversity of fatty acids in non-exposed samples, were more vulnerable to the chemical mixture. Moreover, the species *P. parvum*, *P. tricornutum*, and *Nannochloris* sp., displayed increased lipid production, evidenced as 5–10% increase in lipid fluorescence, after exposure to the chemical mixture. This lipid increase has the potential to alter the intrinsic sensitivity of the populations because storage lipids facilitate membrane repair, reconstitution and may, in the short-term, dilute contaminants within cells. Our study integrated principles of thermodynamics through the assessment of membrane saturation (*i.e.* chemical activity), and a lipid trait-based assessment to elucidate the differences in population vulnerability among phytoplankton species exposed to HOC mixtures.

Received 1st May 2024
Accepted 27th September 2024

DOI: 10.1039/d4em00249k

rsc.li/espi

Environmental significance

Hydrophobic organic contaminants accumulate in phytoplankton and impact cell membrane functionality and population growth. We demonstrate that the sensitivity to chemical pollution among five tested phytoplankton species differed significantly, despite confirmation of comparable internal chemical activities across species. Our results suggest that species-inherent differences in energy storage and lipid production play an important role for sensitivity to chemical pollution. For instance, the two species with the strongest effects on population growth had higher lipid content and significantly different lipid composition compared to the other three species. Our results demonstrated that the same level of chemical pollution may lead to altered composition of phytoplankton species in surface waters, with potential consequences for ecosystem functionality and productivity.

1. Introduction

The increasing production of chemicals and their complex interactions with biological systems challenge current risk assessment procedures.[1] Consequently, aquatic ecosystems are exposed to diverse chemicals emitted into the environment, including hydrophobic organic contaminants (HOCs). HOCs encompass organic compounds such as polycyclic aromatic hydrocarbons (PAHs) and polychlorinated biphenyls (PCBs), which have low solubility in water due to their hydrophobic

[a]*Department of Environmental Science, Stockholm University, Sweden. E-mail: Talles.Oliveira@aces.su.se*

[b]*Department of Biology and Environmental Science, Centre of Ecology and Evolution and Microbial Model Systems (EEMiS), Linnaeus University, Sweden*

[c]*Department of Ecology, Environment and Plant Sciences, Stockholm University, Sweden*

† Electronic supplementary information (ESI) available. See DOI: https://doi.org/10.1039/d4em00249k

nature.[2] Consequently, HOCs tend to partition to suspended particulate organic matter in water, including phytoplankton cells that are rich in lipid-rich biological membranes.[3] The effects of HOCs in phytoplankton are observed across various metabolic, biochemical, and structural endpoints, such as population growth, photosynthesis, enzyme activity, gene expression, and protein synthesis, ultimately leading to alterations in population abundance and community structure.[4–6] Hence, chemical pollution can directly impact phytoplankton functionality and ecosystem services, with implications for the aquatic food web[7] and oceanic carbon cycling and productivity.[8]

The uptake of freely dissolved HOCs by phytoplankton is a passive process, driven by the physicochemical properties of the chemicals and the cell's capacity to dissolve and store these substances.[9] Factors such as the contaminant's affinity for the specific cell matrix and the concentration of the chemical influence both the toxic response and the intrinsic sensitivity of an organism to chemical exposure.[10] HOCs partition into the lipid membranes of the cell, causing alterations of membrane permeability and thereby interferences in membrane-associated processes such as photosynthesis and transport of metabolites in and out of the cell.[11,12] These effects are primarily related to the presence of the contaminant molecule in the membrane rather than the chemical structure of the compound itself. This type of toxicity is therefore called non-specific toxicity. While every compound has the potential to exert non-specific toxicity and cause disturbances of biological membranes, this mode of action is often referred to as baseline toxicity.[11,13] Although it is compound-independent, HOCs contribute the most to baseline toxicity, as they are poorly water soluble and instead have a high affinity for lipids.[2]

The extent of physical damage on the cellular membrane, and the level of membrane saturation by a contaminant are intricately linked. The ratio between the concentration of a chemical and its maximum solubility in a given matrix provides the relative saturation, which, in turn, approximates a compound's chemical activity.[14] Gradients of chemical activity are thereby governing the potential for spontaneous physicochemical processes like diffusion and partitioning of the chemical to other matrices, such as into a phytoplankton cell or within that cell.[2]

Baseline toxicity is additive.[15] Applying the additive principle of effects caused by mixtures of chemicals allows for the prediction of responses, such as growth inhibition in phytoplankton populations, through dose–response curves,[14,16] where the additive dose of the mixture is accounted for. Similarly, the chemical activity approach can be applied to mixtures of HOCs, as the chemical activity of individual chemicals is also additive, and linked to baseline toxicity. In this scenario, equivalent chemical activities, whether originating from single compounds or mixtures, are anticipated to yield the same level of membrane saturation and the corresponding baseline toxicity.[17,18] Based on the established link between chemical activity and baseline toxicity,[16,17] it should theoretically be possible to predict the effects caused by a certain level of membrane saturation. Yet, the vulnerability of phytoplankton populations to chemical pollution at non-acute toxicity levels appears to vary across species in both concentration- and chemical activity-based assessments.[16,18,19] According to Van Straalen's (1994) vulnerability model,[20] a chemical's ecotoxicological effects on populations are categorized as external exposure, intrinsic sensitivity and population sustainability.[21] In our study, external exposure is controlled through passive dosing for the entire exposure period, ensuring observed effects are confidently linked to pre-set and controlled chemical activities. Any sensitivity differences can then be primarily attributed to population sustainability (*i.e.* demographic traits such as growth rate) and intrinsic factors determining how the chemical moves within the organism (toxicokinetic) and how the chemicals interact with the biological systems (toxicodynamic).

The evolutionary adaptation history of phytoplankton species leads to diverse functional traits like lipid composition, cell size, toxin production, and growth rate, with lipid content and composition being particularly crucial for bioaccumulation of HOCs, internal distribution, and mode of action.[22,23] The role of lipid content and profile for phytoplankton sensitivity is multifaceted and can influence various aspects of the response to organic contaminants.[24] First, phytoplankton species naturally exhibit variations in lipid classes and composition due to their adaptive strategies and nutritional status.[25] Second, the interplay between HOCs and lipid metabolism is dynamic, and biological responses involving the synthesis, breakdown, and modification of lipids within algal cells respond quickly to chemical stressors.

Previous studies have demonstrated that PAHs function well as models for HOCs in chemical activity-based research,[17,26–29] making them suitable for experimental research on the effects of chemical mixtures on aquatic life. Based on the assumption of additivity and the non-dependence on individual chemical identities within the mixture, the effects observed from PAH mixtures and their chemical activities can be extended to other HOC mixtures.[14,30]

Here, we aim to investigate how five phytoplankton species from different eukaryotic groups, each with varying growth rates and natural variations in lipid classes and composition, respond to the same range of chemical activities of a PAH mixture. We thereby address the environmental chemistry paradigm on how membrane saturation links to not only baseline toxicity but also ecological effects. We hypothesize that although there is a dose–response relationship between effect and chemical activity for each individual species, phytoplankton traits will contribute to sensitivity variations and lead to species differences in population vulnerability. Specifically, we hypothesize that phytoplankton populations with high lipid content will be more affected by chemical mixtures.

2. Material and methods

2.1. Chemicals and materials

This study employed four PAHs to produce the chemical activity ranging from 0.02 to 0.17. The selected PAHs were acenaphthene (referred to as Ace, CAS 83-32-9, lot MKCG4614), phenanthrene (referred to as Phe, CAS 85-01-8, lot MKCG9999), fluorene (referred to as Flu, CAS 86-73-7, Lot STBJ0395), and

fluoranthene (referred to as FluO, CAS 206-44-0, Lot MKCF7378). All PAHs were procured from Sigma-Aldrich, Copenhagen, Denmark. For the preparation of saturated solutions, we utilized methanol (HPLC-grade, LiChrosolv®, Merck KGaA, Germany). *n*-hexane (Supra Solv®, Merck) was used for extraction of PAHs from biota. Translucent silicone cords made of polydimethylsiloxane (PDMS) (product code 136-8380, 3 mm diameter, AlteSil™, Altec®, England) were used as a passive dosing donor. Ethyl acetate and ethanol were used for silicone cleaning, and Millipore Water (Milli-Q®, Sigma-Aldrich) for rinsing.

2.2. Mixture preparation, silicone loading and passive dosing

PAH-methanol suspensions were prepared for each of the four PAHs by oversaturating methanol with PAH crystals using amber scotch glass bottles.[17] The chemical activity of the PAH-methanol suspensions was calculated based on the compound's melting point and approximating the entropy of melting as 56 J mol^{-1} K^{-1} (Walden's rule) using the eqn (1):

$$a_{max} = \exp 6.8\left[1 - \frac{T_m}{T}\right] = \frac{S_s}{S_L} \quad (1)$$

where a_{max} is the maximum chemical activity in solution (unitless), T_m is the melting point (K) of each PAH, and T is the exposure temperature (290 K).[17,28] Alternatively, the maximum activity can be estimated by the ratio of the solubility of the PAH compound (S_s) and its aqueous subcooled liquid solubility (S_L), both at the exposure temperature.[31,32] The saturated methanol solutions were combined to prepare mixtures of PAHs at four different chemical activities (0.02, 0.06, 0.09, and 0.17). The chemical activity range was chosen to cover the previously observed baseline toxicity interval of chemical activity (0.01–0.1)[33] and an additional high level (0.17) to ensure a complete dose–response curve for less vulnerable species populations.

Translucent silicone cords made of polydimethylsiloxane (PDMS) (product code 136-8380; 3 mm diameter; AlteSilTM, Altec®, England) were cleaned with deionized water, ethyl acetate, and ethanol, and then cut into one-gram pieces.[34] The cleaned silicone pieces were placed in amber scotch bottles containing the PAH mixture and allowed to equilibrate by partitioning at room temperature (25 °C) for at least 48 h at a bench shaker. After removing the methanol solution, the silicone pieces were washed with Milli-Q water. The silicone pieces were distributed into scintillation vials, with one gram of silicone per vial. The loaded silicones pieces were stored in the vials with Milli-Q water at −20 °C until exposure.

2.3. Test organisms and algae cultures

Four phytoplankton species were tested: *Monoraphidium minutum* (Chlorophyceae, KAC 90, sphere 5–10 μm), *Prymnesium parvum* (Haptophyta, Coccolithophyceae, KAC 39, oval shape 10–12 × 5 μm), *Phaeodactylum tricornutum* (Bacillariophyta, CCMP 2928, elongated oval 10 × 3 μm), and a picoeucaryote species (KAC119, sphere 2 μm). The closest relative of KAC 119 based on 18S rRNA sequence is *Nannochloris* sp.[35] (Trebuoxiophyceae). Additionally, growth inhibition data for *Rhodomonas salina* (Chryptophyceae, KAC 30) from Oliveira dos Anjos *et al.*, (2023)[36] were incorporated into this study. All cultures were obtained from the Kalmar Algae Collection (Linnaeus University, Sweden). The stock cultures were maintained in f/2 medium (Guillard, 1975) at 7 psu at a light intensity of 80–100 μmol photons m^{-2} s^{-1}, 16 : 8 light–dark cycle and at 16 °C. In the case of *P. tricornutum*, silica was added to the medium.

2.4. Experimental design

Intermediate cultures of the phytoplankton species were generated and maintained at the same conditions as previously described in this study, with the exception of the temperature, which was adjusted to 17 °C. These intermediate cultures served two purposes at different stages in this study (Fig. 1). First, large volumes of culture (*i.e.* spherical glass bottle of 1 L, $n = 3$) were used to generate enough biomass for total lipid quantification and characterization of lipid profiles (*i.e.* lipidomic, bound and free fatty acids) (Fig. 1). Culture growth was monitored using an OD750 (UV-Vis PC1600) spectrophotometer. Additional nutrients (f/2 based) were added on day 4, along with daily additions of 1 g L^{-1} sodium bicarbonate, and the biomass harvesting took place on day 6. Algal cells were harvested from the algal cultures by centrifugation at 10 500×*g* (Beckman Avanti j-25) and washed with 0.1 M ammonium formate. Then, the collected biomass was stored at −20 °C and later dried using SvanVac freeze dryer. Second, low-volume cultures (200 mL glass Erlenmeyer flasks) were generated for the algae toxicity test (Fig. 1). The populations in exponential growth were exposed to a range of chemical activity, ranging from 0.02 to 0.17, and the effects on growth inhibition, chl *a* autofluorescence, and change in neutral lipids were observed. Growth rates were generated independently for the 1 L intermediate culture ($n = 3$) over six days and at the end of the algae toxicity test for both the control ($n = 3$) and solvent control/PDMS ($n = 3$). Culture growth was expressed as the logarithmic increase in cell density from day 0 (X_0) to day 3 (X_3), as per eqn (2).

$$\text{Growth rate per day } (\mu) = \frac{\ln(X_3) - \ln(X_0)}{\Delta t} \quad (2)$$

The responses in growth inhibition of the cryptophyte *Rhodomonas salina* (KAC 30) to chemical activity (0.009–0.146) were determined previously using the same experimental setup with passive dosing, and the data were incorporated into this study.[36] The growth inhibition test followed the same guideline (OECD 201).[37]

2.4.1. Lipid profile characterization and total lipid quantification. The lipid extraction and lipidomic analysis were performed by the Swedish Metabolic Center (SMC; Swedish University of Agricultural Sciences/Umeå University). Briefly, the lipid extraction followed the Folch method, with stored chloroform extracts at −80 °C for LC-MS analysis. Internal standards were added before extraction, and UHPLC-QTOF/MS analysis was conducted for targeted feature extraction and lipid annotation, with additional fatty acid analysis through

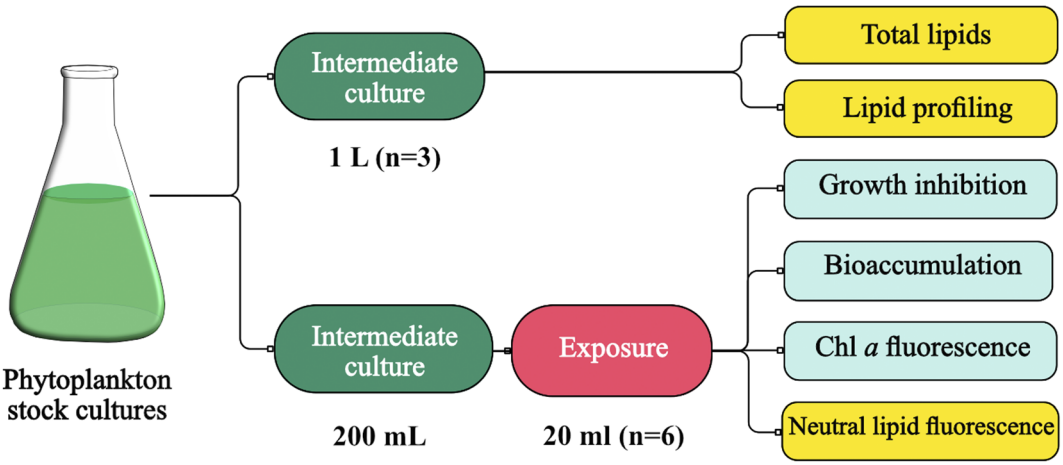

Fig. 1 Phytoplankton cultivation and chemical activity assessment for lipidomic and algae toxicity studies. Figure generated through Canva® and Affinity Design®.

methylation and transmethylation techniques. Further details can be found in Text ESI 1.†

For the analysis of total lipid content (% dry weight), lipids were extracted following a modified Bligh and Dyer method.[38] Dry biomass (100 mg) was mixed with 4.5 mL chloroform : methanol 2 : 1 (v/v), and subjected to vortexing and sonication, and then incubated in the dark at 4 °C overnight and centrifuged at 2800×*g* for 10 minutes. The collected liquid containing extracted lipids was collected, filtered, and dried at 60 °C until a constant weight was achieved.

2.4.2. Algae toxicity test. Before the start of the toxicity test, the stock cultures were prepared 3–4 days in advance to ensure they were in the exponential growth phase at the time of exposure to the chemical mixture. The algae growth inhibition test was based on OECD guideline 201.[37] Deviations from this guideline include the addition of 160 mg L^{-1} of sodium bicarbonate to the exposure medium to minimize the growth inhibition caused by lack of CO_2 observed in closed systems.[39] Before exposure started, the desired inoculum was determined by flow cytometry to give a start density of 4×10^4 cells per mL in each vial (20 mL). Bioassays were performed between November and December 2022, with the exception of *R. salina* (March to May 2022).[36]

Algae cultures were exposed to four different nominal chemical activities (0.02, 0.06, 0.09, and 0.17) for 72 h. Additionally, vials without silicone and vials with silicone loaded with methanol only (solvent control, PDMS) were added as controls. The vials were transferred to a climate control room at the same conditions as described for the stock cultures. All treatments and controls were prepared in six replicates, with one set of triplicates dedicated for growth inhibition, chl *a* autofluorescence, changes in lipid storage, and live/dead test, and the other set of triplicates was used for particulate organic carbon (POC) and PAH quantification.

During exposure, all vials were under constant movement (shaking table, 60 rpm) and their position were randomized and changed every day. Sub-samples of 180 μL were taken from three replicates to measure cell densities at day 0 and after 72 h using a flow cytometer (CyFlow Cube 6, Sysmex, Germany) equipped with red and blue lasers and a standard filter setup. The flow rate was set to 1 μL s^{-1}. Cell densities were obtained by plotting a two-dimensional cytogram. A fixed gate was applied to identify viable cells exhibiting red fluorescence in the 660–700 nm band (chl *a* autofluorescence). This enabled the differentiation of non-algal particles and can be used as a proxy for chl *a* content per cell. Culture growth was expressed as the logarithmic increase in cell density at day 0 (X_0) and day 3 (X_3), as per eqn (2)

To account for any additional effects caused by the silicone, we used the growth rates based on the algae exposed to the solvent control (PDMS) as a reference point to calculate growth inhibition caused by the chemical mixture. In addition, the optical density for all species were recorded. Quality control for the algae toxicity tests is provided in the ESI (Text ESI 2).†

2.4.3. Lipid changes measured with BODIPY fluorescence. To assess changes in intracellular lipids in exposed phytoplankton (Fig. 1), we employed the lipophilic fluorescent dye BODIPY 505/515 (4,4-difluoro-1,3,5,7-tetramethyl-4-bora-3a,4a-diaza-*s*-indacene; Invitrogen Molecular Probes, Carlsbad, CA). BODIPY can stain a wide range of lipids, including fatty acids, phospholipids, cholesterol esters, and ceramides. BODIPY does not enable separation of different lipids from each other. The measured fluorescence is primarily associated with lipid droplets within the cells, predominantly over membrane signals. Therefore, changes in fluorescence were used as a proxy for alterations in neutral storage lipids. BODIPY was prepared in DMSO to achieve a working solution of 0.134 μg mL^{-1} and stored in the dark at −20 °C. 400 μL of BODIPY working solution was added to 400 μL algae sample resulting in a 0.067 μg mL^{-1} final concentration.[40] All samples were incubated for 10 minutes at room temperature. Fluorescence intensity was detected by flow cytometry using a 488 nm band excitation filter and a 525 nm emission filter. The relative fluorescence intensity (arbitrary units) was calculated by subtraction of autofluorescence of the algae in the non-stained samples from the fluorescence of BODIPY-stained samples. The staining test with BODIPY was not performed on *R. salina*.

2.4.4. Live and dead cell staining. Subsamples were incubated with SYTOX Green (0.5 μM, 15 min, Invitrogen, Life Technologies). This stain can only enter cells with compromised membranes. Upon binding to DNA, SYTOX Green exhibits an excitation maximum of 504 nm and an emission maximum of 523 nm. Cells were categorized as live or dead based on criteria such as red chlorophyll fluorescence without green DNA fluorescence or red chlorophyll fluorescence with green nuclear fluorescence. Forward and side light scatter measurements were also utilized to aid in the assessment of the target cell populations.

2.5. Exposure confirmation

2.5.1. Chemical activity in water. The chemical activity in the medium during the exposure was estimated based on the PAHs' freely dissolved concentrations in equilibrated Milli-Q water after exposure.[36] At the end of the exposure, the medium was discarded, and the vials containing the loaded silicone were rinsed with Milli-Q water. Subsequently, the vials were filled with 20 mL of Milli-Q water and left to equilibrate in the dark at room temperature (25 °C) for 48 hours on a shaker platform. After equilibration, an aliquot of 750 μL was taken from each sample and mixed with 750 μL of acetonitrile. PAH determination in the equilibrated Milli-Q water samples was performed using high-performance liquid chromatography coupled to a photodiode array detector (HPLC-PDA). Chromatographic separation was achieved on a HALO 90 Å PAH column, with the mobile phases Milli-Q water and acetonitrile. The samples were analyzed directly after vortexing, and quantification was carried out using an external calibration curve. Further details are provided in the Text ESI 3,† including specific wavelengths used for PDA detection, the temperature-solubility adjustment method for PAHs in water and quality control and assurance (Table ESI 1†).

2.5.2. Chemical activity in biota. Bioaccumulation of PAHs in the algae was quantified as concentrations of PAHs normalized to particulate organic carbon content (POC). All samples were spiked with a 10 μL solution containing 7.5 ppm of deuterated internal standards (Ace-d10, Phe-d10, Flu-d10, and FluO-d10). Extraction was carried out in *n*-hexane using an ultrasonic processor (VCX 750, Sonics, Newton USA), coupled with a 1/8″ microtip (450 watts, amplitude 35%, pulse 02/03, 5 min) and for 20 min in an ultrasound bath (Ultrasonic Cleaner, USC-TH, VWR). Following phase separation with water, the supernatant was collected, reduced to 0.5 mL, and purified through a silica column with 10% deactivation. The eluent was concentrated to 100 μL under gentle N_2-stream. PAH quantification was performed *via* Gas Chromatography-Mass Spectrometry (GC-MS) utilizing a nine-point calibration curve alongside internal standards. To determine particulate organic carbon content in the algae (POC), samples of 10 mL culture were filtered on pre-combusted (475 °C, 2 h) glass fibre filters (GF/F 25 mm Advantec®). The filters were dried (60 °C overnight) and carbon content measured as release of CO_2 after combustion at 920 °C on an Elemental Analyzer (PerkinElmer 2400). Quality control and assurance for the PAH quantification in biota are displayed in the Table ESI 2.† Some of the samples did not meet the QC limits (±25% in the recovery). These values should thus be interpreted carefully.

The concept of chemical activity in exposure and effect studies relies on the thermodynamic equilibrium of the studied chemicals across various compartments within the exposure system, including the medium, silicone, and biota. We used literature values on organic carbon-water equilibrium partition ratios (K_{oc}) to calculate the chemical activity in the exposed algae, using the concentrations we determined in algae POC. The chemical activity in the algae could then be compared with the chemical activity in the water (medium), and if similar, the system was considered to be in equilibrium. Observations of K_{oc} values for a single chemical vary depending on the characteristics and thus sorption properties of the organic carbon. Therefore, we calculated chemical activities in the biota using four different K_{oc} values[41–44] and compared them with the measured chemical activity of the medium. For this, chemical activities (a_{biota}) were calculated for the POC-normalized concentrations in the algae (C_{biota}) using eqn (3). The aqueous subcooled liquid solubility of the PAHs is represented by $S_{L\ water}$.

$$a_{biota} = C_{biota}\ (mg\ kg^{-1}) / S_{L\ water}\ (mg\ L^{-1}) \times K_{oc}\ (L\ kg^{-1}) \quad (3)$$

2.6. Statistics and data analysis

Principal component analysis (PCA) was performed on the lipidomic data (peak areas) as well as on the concentrations of free and bound fatty acids. This analysis aimed to visualize the general 2D clustering, group the species according to their lipid profile, and identify the groups of lipids and fatty acids that contribute the most to the observed pattern. The normalized response for growth inhibition observed in exposed cultures was plotted against chemical activity, and a sigmoidal dose–response curve was fitted to the log-transformed chemical activities, enabling the calculation of the effective chemical activity that causes 50% effect (Ea_{50}). The variable slope model derived the Hill Slope from the data set. The highest chemical activity in the experiment (0.17) resulted in a maximum of 47% growth inhibition in *P. tricornutum*, highlighting its tolerance. To generate an inhibition curve for this species, the effect was extrapolated to 100% at 0.3 chemical activity. Additionally, chl *a* autofluorescence per cell and change in neutral lipids per cell were compared to the control.

The growth inhibition curves were generated from flow cytometry data for *M. minutum*, *P. parvum*, *P. tricornutum*, and from optical density for *R. salina* and *Nannochloris* sp. For *R. salina*, no data from flow cytometry was available, whereas for *Nannochloris* sp. optical density exhibited lower variation compared to the flow cytometry data. An unpaired *t*-test was performed to analyze the differences in growth rate between the intermediate and post-exposure cultures. One-way ANOVA was conducted to assess differences in total lipids, and Tukey's post-hoc test was employed to analyze differences across species. Additionally, one-way ANOVA was used to evaluate differences in chl *a* autofluorescence per cell, change in neutral lipids, change in POC (ugC/cell), and mortality between the levels of chemical

activity and a reference (control or PDMS only treatment). All statistical analyses and graphs were performed and constructed using GraphPad Prism® version 9.4 (San Diego, CA).

3. Results and discussion

We assessed the vulnerability of five different strains of phytoplankton populations to chemical activity and the role of lipids for the observed vulnerability using the framework for traits-based assessment in ecotoxicology,[21] based on the vulnerability conceptual model of Van Straalen (1994)[20] (Fig. 2). First, a dose–response curve was established between growth inhibition and different levels of chemical activity of a PAH mixture, showing differences in population vulnerability (Section 3.1). Second, we evaluated the three categories in Van Straalen's model that describe the ecotoxicological effect of a chemical mixture on populations. The categories of the model are external exposure, intrinsic sensitivity and population sustainability (Fig. 2). External exposure was controlled using passive dosing, and the measured activity in biota indicated that the system reached equilibrium (Section 3.1). Therefore, the differences in vulnerability observed in the five tested phytoplankton species reside in the other two aspects of the model: population sustainability (Section 3.2) and intrinsic sensitivity (toxicokinetic and toxicodynamic) (Section 3.3) (Fig. 2).

3.1. Differences in population vulnerability

The five analyzed phytoplankton species exhibited distinctly different lipid content and growth rates in the intermediate culture (Table 1). All algae species displayed exponential growth in the control across all tests, with specific growth ranging from 0.42 days^{-1} for *R. salinas* to 0.56 days^{-1} for *P. tricornutum* (Table 1). pH increased in all samples following biomass growth, as indicated in Table ESI 3.†

The chemical activity of the PAH mixture for both medium and algae (biota) showed a linear and positive correlation (Fig. 3 A–E). Most of the predicted chemical activities in algae were close to the equilibrium line strongly indicating that the system was in equilibrium, and thus that chemical activity in the algae mirrored that of the silicone and the exposure medium. In the case of *P. parvum*, the calculated chemical activity in biota was lower than expected for an equilibrium scenario. The data points at the lower chemical activities for *P. parvum* have high uncertainties due to very low amounts of POC, and thus the equilibrium assessment for this species is overall uncertain. Given the long exposure time (72 h) in a closed system, and that our data for the other three species as well as earlier algae data demonstrate equilibrium for also larger HOCs within 25 h,[46] we assume *P. parvum* was close to equilibrium. However, the results for *P. parvum* are more uncertain and need to be interpreted with some care.

Freely dissolved concentrations of PAHs in water, concentrations of PAHs in organic carbon, and quality control and assurance for GC-MS analysis can be found in Tables ESI 1, ESI 4, and ESI 2.†

The response of the five phytoplankton populations varied in relation to the chemical activity range exerted by the PAH mixture. The chemical mixture had an inhibitory effect on the

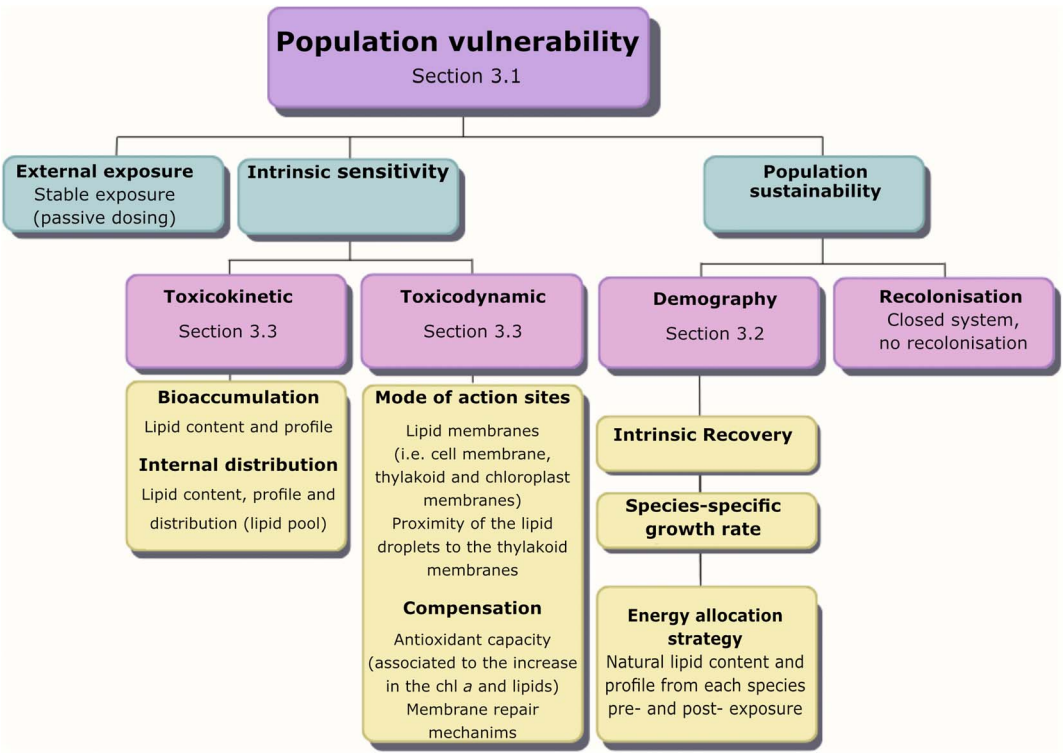

Fig. 2 Categories for the utilization of traits in ecotoxicology (van Straalen 1994[20] see Rubach *et al.*, 2011 [21]) to illustrate lipids as a trait in various processes influencing population vulnerability to chemical exposure.

Table 1 Growth rate and lipid content observed in non-exposed algae and species-specific growth rates in exposed algae

	Intermediate culture (non-exposed) (mean ± s.d., $n = 3$)		Toxicity test (exposed) (mean ± s.d., $n = 3$)	
Species	Lipid content [%]	μ	μ control	μ PDMS
P. parvum	32.8 ± 1.70^{a}	0.44 ± 0.02^{c}	0.53 ± 0.15	0.45 ± 0.14
R. salina	22.1 ± 1.23^{b}	0.48 ± 0.02^{c}	0.42 ± 0.02	0.45 ± 0.03
M. minutum	19.7 ± 0.43^{bc}	0.56 ± 0.01^{b}	0.49 ± 0.06	0.69 ± 0.13
P.tricornutum	18.3 ± 0.89^{c}	0.68 ± 0.02^{a}	0.56 ± 0.19	0.47 ± 0.05
Nannochloris sp	14.8 ± 0.43^{d}	0.58 ± 0.00^{b}	0.43 ± 0.01	0.49 ± 0.01*

(μ) The specific growth rate d^{-1}. (*) Significant difference between control and PDMS. Different letters indicate significant differences ($p < 0.05$) between treatments according to the Tukey's post-hoc test.

growth for all species populations, with *P. parvum* showing the highest vulnerability (Fig. 4 A–E). Despite the dose–response curve being constrained to a range of 0–100% effect, the experimental results revealed substantial growth inhibition for *P. parvum*, reaching 123% at 0.09 and 261% at 0.17 chemical activity (Table ESI 5†); demonstrating a decline and not growth reduction of this species population. The other species demonstrated growth, albeit at a reduced rate compared to the control (Fig. 4 A–E, Table ESI 5†). The second dose–response curve (green) in Fig. 4 A–E, based on the predictions for chemical activity in biota (Fig. 3 A–E, Table ESI 4†), was added to the graphs in order to illustrate the alignment between the curve obtained based on the chemical activity in the medium and chemical activity in biota. Except for *P. parvum*, both dose–response curves were closely aligned.

Following *P. parvum*, the vulnerability order, as determined by the effective chemical activity causing 50% growth inhibition (Ea_{50}), was as follows: *R. salinas*, *Nannochloris* sp., *M. minutum* and *P. tricornutum* (Fig. 4 A–E, Table ESI 5†). Although the equilibrium assessment for *P. parvum* was uncertain, this species would still be the most sensitive, with the lowest Ea_{50}. The Ea_{50} of the most sensitive species *P. parvum*, *R. salina* and *Nannochloris* sp., fell within the chemical activity range of 0.01 to 0.1; the chemical activity range with previously reported effects at various trophic levels.[18] The most tolerant species, *P. tricornutum* exhibited effects beyond 0.1 ($Ea_{50} = 0.184$), indicating better tolerance to chemicals causing baseline toxicity compared to the other species. Reductions in POC indicate a similar vulnerability ranking at the highest chemical activity with a shift between *Nannochloris* sp. and *M. minutum* (Table ESI 6†). Previous research has documented tolerance of marine diatoms such as *P. tricornutum* to HOCs. For instance, Niehus *et al.* (2018)[16] calculated an Ea_{50} of 0.14 for this species. The mechanism behind the tolerance of *P. tricornutum* and other diatoms to baseline toxicants remains unclear. However, it has been suggested that the capacity of diatoms to maintain membrane stability contributes to population recovery after exposure, as previously demonstrated in the diatom *Nitschia brevirostris*.[47]

From a thermodynamic perspective, and given the established correlation between chemical activity and baseline toxicity and that the membranes of the five tested species reached similar levels of relative saturation. Comparable effects at the cellular level would be expected. However, in agreement with our hypothesis, sensitivities of the tested phytoplankton varied. Growth inhibition is a multifaceted endpoint assessed at population level, involving not only the partitioning of chemicals to membranes in individual cells but also encompassing biological responses such as alterations in lipid content, pigment synthesis and breakdown, and antioxidative reactions. This complexity resulted in varying population vulnerabilities among the five phytoplankton species exposed to the same range of chemical activities. In the next sections, we focus on the biological characteristics that modulate the population sustainability (3.2) and intrinsic sensitivity (3.3), with a specific focus on lipid content and profile as trait for the population vulnerability assessment (Fig. 2).

3.2. Species-specific growth rate

P. parvum displayed the highest lipid content, surpassing *Nannochloris* sp. – the species with the lowest lipid content – by more than a factor of two in the intermediate cultures (Table 1). Both *P. parvum* and *R. salina* showed lower growth rates compared to the other three species grown under optimum conditions (Table 1, Fig. ESI 1†). *M. minutum*, *P. tricornutum*, and *Nannochloris* sp. showed lower lipid content in that order, accompanying faster growth rates compared to *P. parvum* and *R. salina*. Notably, distinct variations in lipid composition distinguished *P. parvum* and *R. salina* from the remaining three species, with both species not only exhibiting higher lipid content but also displaying unique characteristics in their lipid profiles (Fig. 5, Fig. ESI 2, Text ESI 4, Table ESI 7–10†).

Despite *P. parvum* and *R. salina* having higher lipid content (Table 1) and a diverse range of polyunsaturated fatty acids (PUFAs) (Fig. 5A–C), they did not demonstrate a significant advantage over the species with lower lipid content in the dose–response curves (Fig. 4A and B); in fact, they were more sensitive. The natural variations in lipid content and profiles observed in the five tested phytoplankton species may offer insights into their distinct strategies for energy utilization. The intrinsic lipid metabolism inherent in each species, shaped by their adaptation history, indicate how these species have been allocating energy to cell reproduction and storage from an evolutionary perspective.[48] The high lipid content and diverse

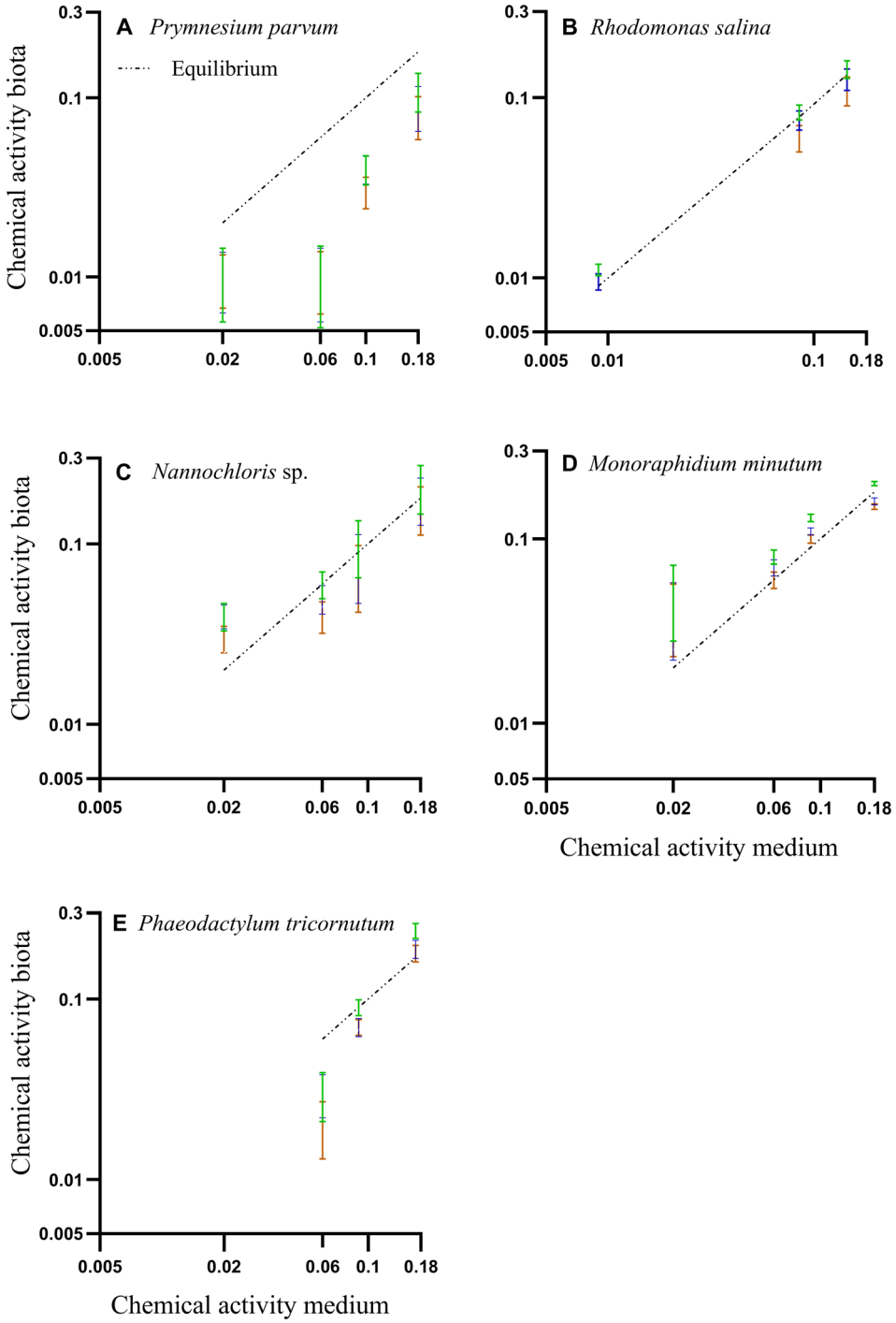

Fig. 3 (A–E) Correlation between PAH chemical activities based on the freely dissolved concentrations in water and biota concentrations. Colored bars are the mean of chemical activities and their respective standard deviations in the biota, calculated from three different organic carbon-water partition ratios (K_{oc}) from literature. Green: Szabo *et al.* 1990.[45] Blue: Di Toro, 1985;[43] Orange: Burgess *et al.*, 2012.[41] The dashed line represents the 1 : 1 line assuming equilibrium.

fatty acids found in *P. parvum* and. *R. salina* indicated that these two species allocate significant amounts of energy towards storage and synthesis of lipid-metabolites rather than growth (Table 1, Fig. 5). Conversely, *P. tricornutum* allocated more energy to population growth rather than synthesis and storage of lipids (Table 1, Fig. 5), exhibiting advantages in sustaining populations during the algae toxicity test (Fig. 4). Species-specific growth rate is accounted for in the overall growth inhibition test (Fig. 4), where the growth rates in the treatments are normalized to the control. Populations of *P. parvum* and. *R. salina* with low growth rate were more vulnerable to the chemical mixture than *P. tricornutum* which had a higher growth

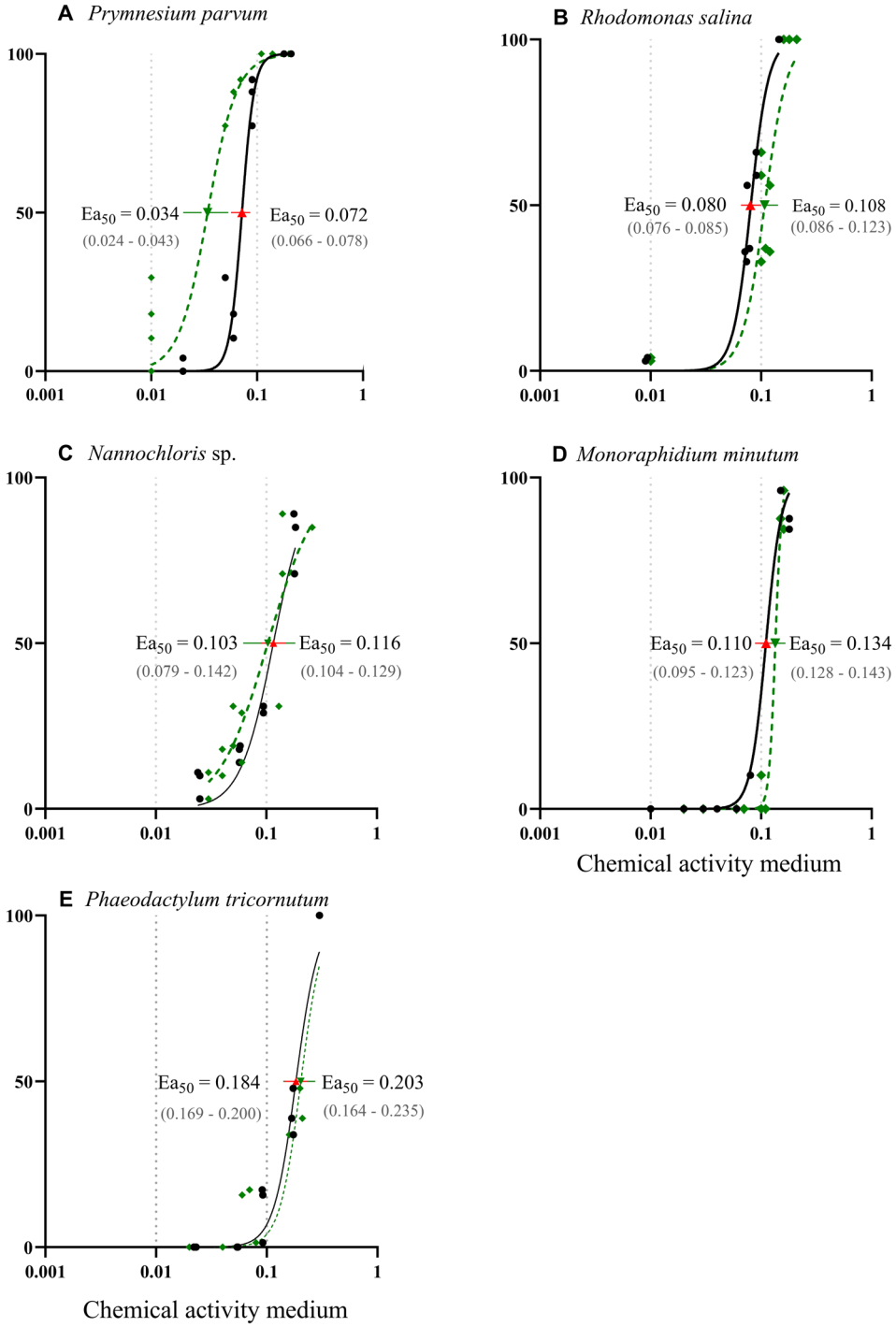

Fig. 4 (A–E) Dose–response curves illustrating effects of chemical activity caused by a PAH mixture on the growth of five algae species. The black solid line represents a sigmoidal curve regression on the relative percentage of growth inhibition over three days, determined by cell abundance measured with a flow cytometer (except for *Nannochloris* sp. and *Rhodomonas salina*,[36] for which optical density was used). The response curve for *P. tricornutum* was extrapolated to a 100% effect at a chemical activity of 0.3. The dashed green line illustrates the chemical activities based on the PAH concentrations in biota. Effective activity that causes 50% of growth inhibition (Ea_{50}) was calculated based on both chemical activity in the medium (red triangle) and biota (green triangle) with their respective 95% confidence interval. Dotted grey lines indicate the range of commonly observed baseline toxicity.

(Table 1, Fig. 4 and 5). Our results point out lipid content and profile as factors which may be influencing species-specific growth rate; a key process for intrinsic recovery and demography (Fig. 2), ultimately modeling population vulnerability.

3.3. Intrinsic sensitivity

For *P. parvum* at all levels of chemical activity, and *P. tricornutum* up to 0.09 chemical activity, the mean chl *a* autofluorescence per cell increased with chemical activity (Fig. 6A and B). This

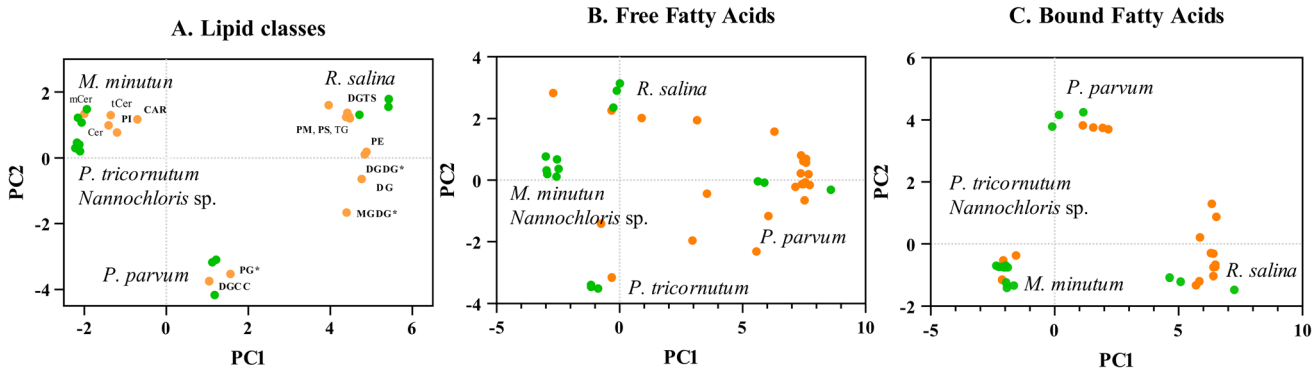

Fig. 5 Lipid content and profile for five phytoplankton species. (A–C): Principal component analysis (PCA) of lipid classes and fatty acids. (A): Classification of 441 metabolites into 16 lipid classes. PC1 + PC2 = 74.6% of variance. (B): Free fatty acids obtained through methylation (ng mg^{-1}) PC1 + PC2 = 77.7% of variance. (C): Bound fatty acids obtained through transmethylation (ng mg^{-1}) PC1 + PC2 = 78.5% of variance. Analysis based on *trans*-methylated samples (ng mg^{-1}). PC scores are represented by orange dots associated to the lipid classes and fatty acids. Loadings are represented by green dots and are associated to the species (n = 3). Phospholipids (in bold): phosphatidylinositol (PI), cardiolipin (CAR), phosphatidylglycerol (PG), phosphatidylmethanol (PM), phosphatidylserine (PS), phosphatidylethanolamine (PE), di-galactosyldiacyl-glycerol (DGDG), di-galactocyl-diacylglycerol (DGCC), diacylglycerol (DG), monogalactosyldiacylglycerol (MGDG), di-acylglyceryl-trimethyl-homoserine (DGTS), di-acylglyceryl-carboxyl-hydroxy-methylcholine. Neutral lipids: monohexosylceramide (mCer), ceramide (Cer), trihexosylceramide (tCer), triglyceride (TG).

pattern was also observed in *R. salina*, where not only an increase in the chl *a* content occurred, but also a reduction in the relative efficiency of this pigment was noted.[36] The increase in chl *a* content in response to stress has been proposed as a response of the algae to enhance photosynthetic efficiency by increasing CO_2 fixation and optimize carbon allocation to carbohydrates and lipids.[49–51] The increase has also been hypothesized as a potential compensatory mechanism reducing accumulated ROS.[52,53] However, further investigations are required to ascertain if a similar compensatory mechanism exists in response to HOC exposure. Like other HOCs, PAHs do not primarily act as photosynthetic inhibitors. Instead, they impact the membrane integrity of chloroplasts and thylakoids leading to baseline toxicity and subsequent secondary effects on electron transport in the photosystem II (PSII).[49,54,55] In other words, the efficiency of the cell to convert light into energy is hampered, resulting in the formation of reactive oxygen species (ROS). These ROS target membranes, including thylakoid lipids, leading to membrane destruction, growth reduction and diminished photosynthesis efficiency.[51,56,57]

P. parvum, *P. tricornutum* and *Nannochloris* sp. showed an increase in their neutral lipid content in response to chemical activity (Fig. 6C). For *P. tricornutum* and *Nannochloris* sp, we observed a significant increase in the neutral lipid content only at the highest chemical activity (0.17). *M. minutum* was the only species that lost carbon content during exposure, likely caused by the reduction in lipid content and high mortality (Fig. 6C and D). *P. parvum* being the most sensitive species (Fig. 4), not only had the highest lipid content (Table 1), but also displayed the earliest response in increasing lipid content when exposed to the chemical mixture (Fig. 6D and E). Although the specific types of fatty acids generated by *P. parvum* after exposure are unknown, this species allocated a substantial amount of energy to shift from biomass production (*i.e.*, population growth) to energy storage metabolism in response to chemical pollution.[58,59]

We could not observe any population-level advantage from an increase in chlorophyll *a* autofluorescence per cell or from an increase in neutral lipids per cell in minimizing growth inhibition. Still, the observed increase in lipid content, triggered by the chemical mixture, indicates the species' capacity to mitigate stress through membrane repair mechanisms and reconstitution (toxicodynamic). In principle, increased lipid content is considered as a mechanism to reduce oxidative stress.[47] The increase in intracellular lipids can enable the maintenance of the redox homeostasis, serving a dual purpose: these molecules act like a sink or buffer for the contaminants (toxicokinetic) and reduce the damage caused by ROS (toxicodynamic). Storage lipids such as triglycerides contain certain fatty acids, particularly PUFAs, crucial for the structural integrity of cell membranes and function as antioxidants, countering free radical formation during photosynthesis.[60] Consequently, triacylglycerols (TAGs) rich in PUFAs could contribute specific compounds essential for promptly restructuring membranes (Table ESI 11†). It remains plausible that some advantages offered by an increase in the lipid content and perhaps chl *a* may become relevant in a post-stress scenario.

Taken together, the tested populations, despite showing a pronounced increase in neutral lipids and chlorophyll *a* autofluorescence, did not exhibit reduced susceptibility to growth inhibition caused by the chemical mixture. Although increases in the chl *a* autofluorescence and increase in neutral lipids which are compensatory mechanisms with implications for intrinsic toxicity (toxicokinetic and toxicodynamic), their detection may not always translate to a significant effect at the population level in the time scale of the experiment. It is also plausible, that the energy expenditure required for these mechanisms can counterintuitively reduce population growth. In our study, the passive donor continuously supplied the medium with PAHs, maintaining the system in equilibrium and potentially surpassing cellular adaptive mechanisms. The

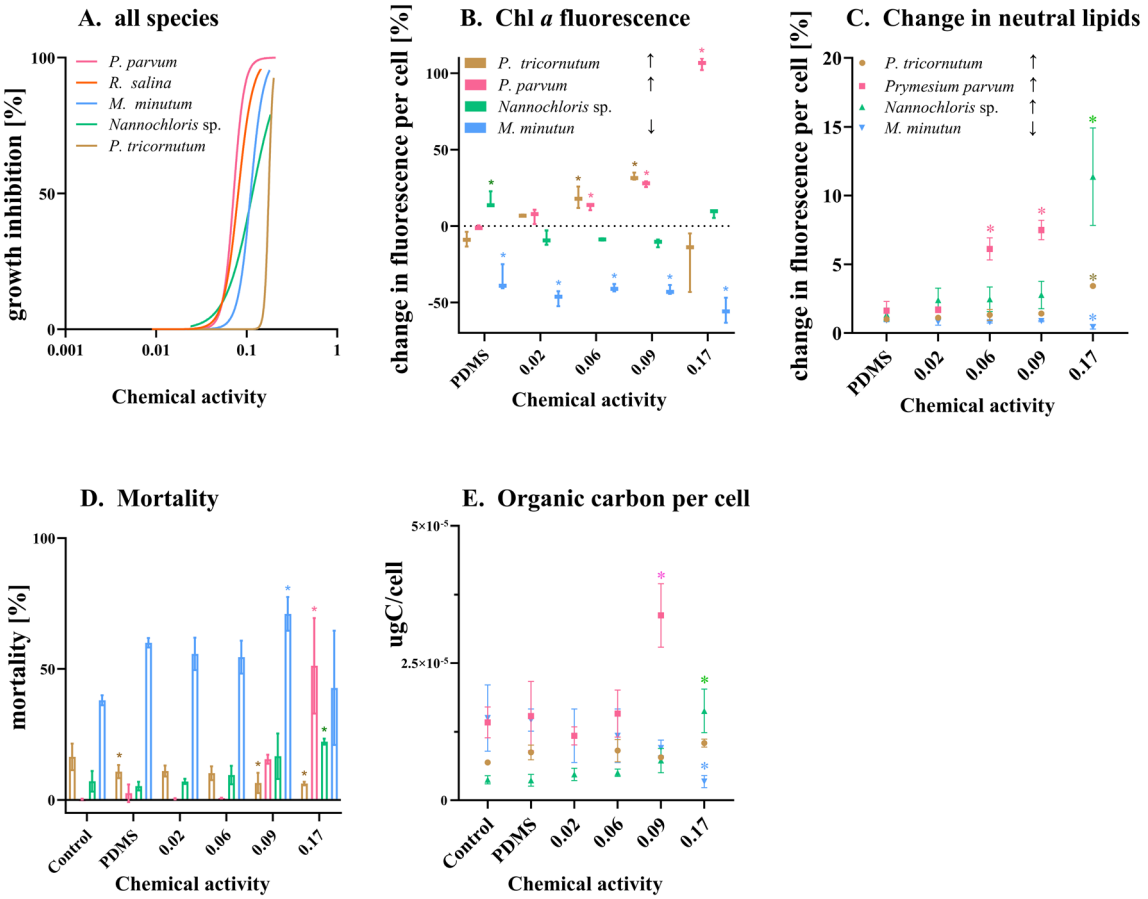

Fig. 6 Effects of a chemical mixture at different chemical activities on algae species (A): dose response curve for five algae species. (B): change in the mean chlorophyll *a* autofluorescence (670 nm) per cell relative to the control (C): neutral lipid content of different algae species measured indirectly at 525 nm fluorescence of lipids stained with BODIPY and expressed as a change in fluorescence per cell relative to the control as a function of the mixture chemical activity. (D): percentage of dead cells stained by the SYTOX GREEN. (E): organic carbon content per cell (ratio between particulate organic carbon and cell density) as function of chemical activity. Means of chl *a* autofluorescence (B) and change in neutral lipids (D) were normalized to the control. Change in total POC was normalized to the solvent control (PDMS). Mortality and organic carbon per cell were not normalized. Error bars represent standard error of mean values. Significant differences of the treatments were assessed by one-way ANOVA. Stars indicate significant differences ($p < 0.05$) between each treatment and a reference (control or PDMS). The arrows indicate the direction of the change (increasing or decreasing).

associated energy cost of these mechanisms could contribute to the overall reduction in population growth.

4. Conclusions

Phytoplankton encounter a myriad of chemicals released into the environment. Hydrophobic organic chemicals accumulate in phytoplankton lipids, impacting the cell membrane functionality, population growth and thereby HOCs have the capacity to affect the cycling of nutrients in aquatic ecosystems. In this study, lipid content and composition were explored as traits to understand the differences in population vulnerability to HOCs among five phytoplankton species from different eukaryotic groups. The phytoplankton populations exhibited varied growth inhibition when exposed to the same range of chemical activities exerted by a PAH mixture. Hence, the five species had comparable levels of membrane saturation of PAHs, while effects varied significantly, demonstrating that growth inhibition encompasses not only the partitioning of the chemical to membranes (thermodynamics), but also the biological characteristics and physiological responses that collectively also modulate population vulnerability. Our study demonstrated how the same level of chemical pollution may alter the composition of phytoplankton species in surface waters. If primary producers are reduced to fewer, more tolerant species with elevated lipid content, their role as vectors of HOCs to higher trophic levels in the aquatic food web may increase in importance. Furthermore, diverse vulnerabilities in the phytoplankton community to chemical pollution may also cause alterations in the functionality and productivity of local aquatic ecosystems.

Data availability

The data supporting this article have been included as part of the ESI.†

Conflicts of interest

There are no conflicts to declare.

Acknowledgements

This work was funded by the Swedish Research Council through VR 2019-03749, Stockholm University – Department of Environmental Science, and FORMAS 2018-00692, SFO Ecochange, and Linnaeus University – Faculty of Health and Life Sciences. We appreciate the help provided by Fredrik Svensson and Anabella Aquilera for providing algal strains used in this study, and Hanna Farnelid and Laura Bas Conn for the support with the flow cytometry analyses. We also thank Zhe Li and Betty Chaumet for assistance with chemical analysis and data quality assurance and Claudia Möckel for assistance with the LC-PDA instrumentation and its maintenance.

References

1 K. Fenner and M. Scheringer, The Need for Chemical Simplification As a Logical Consequence of Ever-Increasing Chemical Pollution, *Environ. Sci. Technol.*, 2021, **55**(21), 14470–14472, DOI: **10.1021/acs.est.1c04903**.

2 R. P. Schwarzenbach, P. M. Gschwend, and D. M. Imboden. *Environmental Organic Chemistry*, John Wiley & Sons, 3rd edn, 2016.

3 D. L. Swackhamer and R. S. Skoglund, Bioaccumulation of PCBs by algae: Kinetics *versus* equilibrium, *Environ. Toxicol. Chem.*, 1993, **12**(5), 831–838, DOI: **10.1002/etc.5620120506**.

4 P. Echeveste, J. Dachs, N. Berrojalbiz and S. Agustí, Decrease in the abundance and viability of oceanic phytoplankton due to trace levels of complex mixtures of organic pollutants, *Chemosphere*, 2010, **81**(2), 161–168, DOI: **10.1016/j.chemosphere.2010.06.072**.

5 P. Echeveste, C. Galbán-Malagón, J. Dachs, N. Berrojalbiz and S. Agustí, Toxicity of natural mixtures of organic pollutants in temperate and polar marine phytoplankton, *Sci. Total Environ.*, 2016, **571**, 34–41, DOI: **10.1016/j.scitotenv.2016.07.111**.

6 H. Ben Othman, F. R. Pick, A. Sakka Hlaili and C. Leboulanger, Effects of polycyclic aromatic hydrocarbons on marine and freshwater microalgae – a review, *J. Hazard. Mater.*, 2023, **441**, 129869, DOI: **10.1016/j.jhazmat.2022.129869**.

7 H. Li, D. Duan, B. Beckingham, Y. Yang, Y. Ran and P. Grathwohl, Impact of trophic levels on partitioning and bioaccumulation of polycyclic aromatic hydrocarbons in particulate organic matter and plankton, *Mar. Pollut. Bull.*, 2020, **160**, 111527, DOI: **10.1016/j.marpolbul.2020.111527**.

8 D. P. Häder and K. Gao, Interactions of anthropogenic stress factors on marine phytoplankton, *Front. Environ. Sci.*, 2015, **3**(MAR), 120191, DOI: **10.3389/fenvs.2015.00014/bibtex**.

9 A. Sobek, Ö. Gustafsson, S. Hajdu and U. Larsson, Particle–Water Partitioning of PCBs in the Photic Zone: A 25-Month Study in the Open Baltic Sea, *Environ. Sci. Technol.*, 2004, **38**(5), 1375–1382, DOI: **10.1021/es034447u**.

10 J. P. Meador, L. S. McCarty, B. I. Escher and W. J. Adams, 10th Anniversary Critical Review: The tissue-residue approach for toxicity assessment: concepts, issues, application, and recommendations, *J. Environ. Monit.*, 2008, **10**(12), 1486–1498, DOI: **10.1039/B814041N**.

11 B. I. Escher and J. L. M. Hermens, Modes of action in ecotoxicology: Their role in body burdens, species sensitivity, QSARs, and mixture effects, *Environ. Sci. Technol.*, 2002, **36**(20), 4201–4217, DOI: **10.1021/ES015848H**.

12 K. Stange and D. L. Swackhamer, Factors affecting phytoplankton species-specific differences in accumulation of 40 polychlorinated biphenyls (PCBs), *Environ. Toxicol. Chem.*, 1994, **13**(11), 1849–1860, DOI: **10.1002/etc.5620131117**.

13 A. P. Van Wezel and A. Opperhuizen, Narcosis due to environmental pollutants in aquatic organisms: Residue-based toxicity, mechanisms, and membrane burdens, *Crit. Rev. Toxicol.*, 1995, **25**(3), 255–279, DOI: **10.3109/10408449509089890**.

14 F. A. P. C. Gobas, P. Mayer, T. F. Parkerton, R. M. Burgess, D. van de Meent and T. Gouin, A chemical activity approach to exposure and risk assessment of chemicals: Focus articles are part of a regular series intended to sharpen understanding of current and emerging topics of interest to the scientific community, *Environ. Toxicol. Chem.*, 2018, **37**(5), 1235–1251, DOI: **10.1002/etc.4091**.

15 P. F. Landrum, G. R. Lotufo, D. C. Gossiaux, M. L. Gedeon and J. H. Lee, Bioaccumulation and critical body residue of PAHs in the amphipod, Diporeia spp.: additional evidence to support toxicity additivity for PAH mixtures, *Chemosphere*, 2003, **51**(6), 481–489, DOI: **10.1016/S0045-6535(02)00863-9**.

16 N. C. Niehus, C. Floeter, H. Hollert and G. Witt, Miniaturised Marine Algae Test with Polycyclic Aromatic Hydrocarbons – Comparing Equilibrium Passive Dosing and Nominal Spiking, *Aquat. Toxicol.*, 2018, **198**, 190–197, DOI: **10.1016/j.aquatox.2018.03.002**.

17 K. E. C. Smith, N. Dom, R. Blust and P. Mayer, Controlling and maintaining exposure of hydrophobic organic compounds in aquatic toxicity tests by passive dosing, *Aquat. Toxicol.*, 2010, **98**(1), 15–24, DOI: **10.1016/j.aquatox.2010.01.007**.

18 F. Reichenberg and P. Mayer, Two complementary sides of bioavailability: Accessibility and chemical activity of organic contaminants in sediments and soils, *Environ. Toxicol. Chem.*, 2006, **25**(5), 1239–1245, DOI: **10.1897/05-458R.1**.

19 S. N. Schmidt and P. Mayer, Linking algal growth inhibition to chemical activity: Baseline toxicity required 1% of saturation, *Chemosphere*, 2015, **120**, 305–308, DOI: **10.1016/j.chemosphere.2014.07.006**.

20 N. Van Straalen, Biodiversity of ecotoxicological responses in animals, *Neth. J. Zool.*, 1994, **441/442**, 112–129, DOI: **10.1163/156854294X00097**.

21 M. N. Rubach, R. Ashauer, D. B. Buchwalter, *et al.*, Framework for traits-based assessment in ecotoxicology, *Integr. Environ. Assess. Manage.*, 2011, **7**(2), 172–186, DOI: **10.1002/IEAM.105**.

22 S. Rizzuto, J. E. Thrane, D. L. Baho, *et al.*, Water Browning Controls Adaptation and Associated Trade-Offs in Phytoplankton Stressed by Chemical Pollution, *Environ. Sci. Technol.*, 2020, **54**(9), 5569–5579, DOI: **10.1021/acs.est.0c00548/asset/images/large/es0c00548_0004.jpeg**.

23 M. H. Medina, J. A. Correa and C. Barata, Micro-evolution due to pollution: Possible consequences for ecosystem responses to toxic stress, *Chemosphere*, 2007, **67**(11), 2105–2114, DOI: **10.1016/j.chemosphere.2006.12.024**.

24 M. J. Kainz and A. T. Fisk, Integrating lipids and contaminants in aquatic ecology and ecotoxicology, *Lipids in Aquatic Ecosystems*, 2009, **9780387893662**, 93–114, DOI: **10.1007/978-0-387-89366-2_5/tables/1**.

25 B. Halling-Sørensen, N. Nyholm, K. O. Kusk and E. Jacobsson, Influence of Nitrogen Status on the Bioconcentration of Hydrophobic Organic Compounds to Selenastrum capricornutum, *Ecotoxicol. Environ. Saf.*, 2000, **45**(1), 33–42, DOI: **10.1006/eesa.1999.1818**.

26 G. E. Bragin, T. F. Parkerton, A. D. Redman, *et al.*, Chronic toxicity of selected polycyclic aromatic hydrocarbons to algae and crustaceans using passive dosing, *Environ. Toxicol. Chem.*, 2016, **35**(12), 2948–2957, DOI: **10.1002/etc.3479**.

27 P. Mayer and M. Holmstrup, Passive dosing of soil invertebrates with polycyclic aromatic hydrocarbons: Limited chemical activity explains toxicity cutoff, *Environ. Sci. Technol.*, 2008, **42**(19), 7516–7521, DOI: **10.1021/es801689y**.

28 E. Rojo-Nieto, K. E. C. Smith, J. A. Perales and P. Mayer, Recreating the seawater mixture composition of HOCs in toxicity tests with Artemia franciscana by passive dosing, *Aquat. Toxicol.*, 2012, **120–121**, 27–34, DOI: **10.1016/j.aquatox.2012.04.006**.

29 N. C. Niehus, C. Floeter, H. Hollert and G. Witt, Miniaturised Marine Algae Test with Polycyclic Aromatic Hydrocarbons – Comparing Equilibrium Passive Dosing and Nominal Spiking, *Aquat. Toxicol.*, 2018, **198**, 190–197, DOI: **10.1016/j.aquatox.2018.03.002**.

30 K. E. C. Smith, S. N. Schmidt, N. Dom, R. Blust, M. Holmstrup and P. Mayer, Baseline toxic mixtures of non-toxic chemicals: "solubility addition" increases exposure for solid hydrophobic chemicals, *Environ. Sci. Technol.*, 2013, **47**(4), 2026–2033, DOI: **10.1021/ES3040472**.

31 F. A. P. C. Gobas, P. Mayer, T. F. Parkerton, R. M. Burgess, D. van de Meent and T. Gouin, A chemical activity approach to exposure and risk assessment of chemicals, *Environ. Toxicol. Chem.*, 2018, **37**(5), 1235–1251, DOI: **10.1002/etc.4091**.

32 P. Mayer and M. Holmstrup, Passive Dosing of Soil Invertebrates with Polycyclic Aromatic Hydrocarbons: Limited Chemical Activity Explains Toxicity Cutoff, *Environ. Sci. Technol.*, 2008, **42**(19), 7516–7521, DOI: **10.1021/es801689y**.

33 S. N. Schmidt, M. Holmstrup, K. E. C. Smith and P. Mayer, Passive dosing of polycyclic aromatic hydrocarbon (PAH) mixtures to terrestrial springtails: Linking mixture toxicity to chemical activities, equilibrium lipid concentrations, and toxic units, *Environ. Sci. Technol.*, 2013, **47**(13), 7020–7027, DOI: **10.1021/es3047813/suppl_file/es3047813_si_001**.

34 H. Birch, R. Hammershøj and P. Mayer, Determining Biodegradation Kinetics of Hydrocarbons at Low Concentrations: Covering 5 and 9 Orders of Magnitude of K_{ow} and K_{aw}, *Environ. Sci. Technol.*, 2018, **52**(4), 2143–2151, DOI: **10.1021/acs.est.7b05624**.

35 Y. Churakova, A. Aguilera, E. Charalampous, *et al.*, Biogenic silica accumulation in picoeukaryotes: Novel players in the marine silica cycle, *Environ. Microbiol. Rep.*, 2023, **15**(4), 282–290, DOI: **10.1111/1758-2229.13144**.

36 T. B. Oliveira dos Anjos, S. Abel, E. Lindehoff, C. Bradshaw and A. Sobek, Assessing the effects of a mixture of hydrophobic contaminants on the algae Rhodomonas salina using the chemical activity concept, *Aquat. Toxicol.*, 2023, **265**, 106742, DOI: **10.1016/j.aquatox.2023.106742**.

37 Test No. 201: Freshwater Alga and Cyanobacteria, Growth Inhibition Test| *OECD Guidelines for the Testing of Chemicals, Section 2 : Effects on Biotic Systems | OECD iLibrary*. Accessed November 20, 2022. **https://www.oecd-ilibrary.org/environment/test-no-201-alga-growth-inhibition-test_9789264069923-en**.

38 E. Bligh, Graham and WJD. A rapid method of total lipid extraction and purificationitle, *Can. J. Biochem. Physiol.*, 1959, **37**(8), 911–917, DOI: **10.1139/o59-099**.

39 D. A. White, A. Pagarette, P. Rooks and S. T. Ali, The effect of sodium bicarbonate supplementation on growth and biochemical composition of marine microalgae cultures, *J. Appl. Phycol.*, 2013, **25**(1), 153–165, DOI: **10.1007/s10811-012-9849-6**.

40 T. Govender, L. Ramanna, I. Rawat and F. Bux, BODIPY staining, an alternative to the Nile Red fluorescence method for the evaluation of intracellular lipids in microalgae, *Bioresour. Technol.*, 2012, **114**, 507–511, DOI: **10.1016/j.biortech.2012.03.024**.

41 R. M. Burgess, S. B. K. Driscoll, M. A. Maynard, R. J. Ozretich, D. R. Mount, and M. C. Reiley. *Equilibrium Partitioning Sediment Benchmarks (ESBs) for the Protection of Benthic Organisms: Procedures for the Determination of the Freely Dissolved Interstitial Water Concentrations of Nonionic Organics.*; 2012. efaidnbmnnnibpcajpcglclefindmkaj/**https://clu-in.org/conf/tio/porewater1/resources/EPA-ESB-Procedures-Determine-freely-dissolved-organics-2012.pdf**.

42 S. W. Karickhoff, Semi-empirical estimation of sorption of hydrophobic pollutants on natural sediments and soils, *Chemosphere*, 1981, **10**(8), 833–846, DOI: **10.1016/0045-6535(81)90083-7**.

43 D. M. Di Toro, A particle interaction model of reversible organic chemical sorption, *Chemosphere*, 1985, **14**(10), 1503–1538, DOI: **10.1016/0045-6535(85)90008-6**.

44 G. Szabo, S. L. Prosser and R. A. Bulman, Determination of the adsorption coefficient (KOC) of some aromatics for soil by RP-HPLC on two immobilized humic acid phases,

Chemosphere, 1990, **21**(6), 777–788, DOI: **10.1016/0045-6535(90)90265-U**.

45 G. Szabo, S. L. Prosser and R. A. Bulman, Determination of the adsorption coefficient (KOC) of some aromatics for soil by RP-HPLC on two immobilized humic acid phases, *Chemosphere*, 1990, **21**(6), 777–788, DOI: **10.1016/0045-6535(90)90265-U**.

46 A. Gerofke, P. Kömp and M. S. McLachlan, Bioconcentration of persistent organic pollutants in four species of marine phytoplankton, *Environ. Toxicol. Chem.*, 2005, **24**(11), 2908–2917, DOI: **10.1897/04-566R.1**.

47 A. N. Croxton, G. H. Wikfors and R. D. Schulterbrandt-Gragg, The use of flow cytometric applications to measure the effects of PAHs on growth, membrane integrity, and relative lipid content of the benthic diatom, Nitzschia brevirostris, *Mar. Pollut. Bull.*, 2015, **91**(1), 160–165, DOI: **10.1016/j.marpolbul.2014.12.010**.

48 C. G. Goodchild, A. M. Simpson, M. Minghetti and S. E. DuRant, Bioenergetics-adverse outcome pathway: Linking organismal and suborganismal energetic endpoints to adverse outcomes, *Environ. Toxicol. Chem.*, 2019, **38**(1), 27–45, DOI: **10.1002/etc.4280**.

49 A. Aksmann and Z. Tukaj, Intact anthracene inhibits photosynthesis in algal cells: A fluorescence induction study on Chlamydomonas reinhardtii cw92 strain, *Chemosphere*, 2008, **74**(1), 26–32, DOI: **10.1016/j.chemosphere.2008.09.064**.

50 J. Shao, G. Yu, Z. Wu, X. Peng and R. Li, Responses of Synechocystis sp. PCC 6803 (cyanobacterium) photosystem II to pyrene stress, *J. Environ. Sci.*, 2010, **22**(7), 1091–1095, DOI: **10.1016/S1001-0742(09)60222-9**.

51 T. W. Jabusch and D. L. Swackhamer, Subcellular accumulation of polychlorinated biphenyls in the green alga Chlamydomonas reinhardtii, *Environ. Toxicol. Chem.*, 2004, **23**(12), 2823–2830, DOI: **10.1897/03-431.1**.

52 S. Chen, L. Wang, W. Feng, *et al.*, Sulfonamides-induced oxidative stress in freshwater microalga Chlorella vulgaris: Evaluation of growth, photosynthesis, antioxidants, ultrastructure, and nucleic acids, *Sci. Rep.*, 2020, **10**(1), 1–11, DOI: **10.1038/s41598-020-65219-2**.

53 A. Mojiri, J. L. Zhou, H. Ratnaweera, S. Rezania and V. M. Nazari, Pharmaceuticals and personal care products in aquatic environments and their removal by algae-based systems, *Chemosphere*, 2022, **288**, 132580, DOI: **10.1016/j.chemosphere.2021.132580**.

54 A. Jajoo. Effects of environmental pollutants polycyclic aromatic hydrocarbons (PAH) on photosynthetic processes. *Photosynthesis: Structures, Mechanisms, and Applications*. Published online May 16, 2017, pp. 249–259. doi:DOI: **10.1007/978-3-319-48873-8_11/COVER**.

55 B. I. Escher, N. Bramaz, J. F. Mueller, P. Quayle, S. Rutishauser and E. L. M. Vermeirssen, Toxic equivalent concentrations (TEQs) for baseline toxicity and specific modes of action as a tool to improve interpretation of ecotoxicity testing of environmental samples, *J. Environ. Monit.*, 2008, **10**(5), 612–621, DOI: **10.1039/B800949J**.

56 A. J. Conner and H. K. Mahanty, Growth responses of unicellular algae to polychlorinated biphenyls: new evidence for photosynthetic inhibition, *Mauri Ora*, 1979, 7, pp. 3–17.

57 L. W. Harding and J. H. Phillips, Polychlorinated biphenyls: Transfer from microparticulates to marine phytoplankton and the effects on photosynthesis, *Science*, 1978, **202**(4373), 1189–1192, DOI: **10.1126/SCIENCE.202.4373.1189**.

58 H. Schuhmann, D. K. Y. Lim and P. M. Schenk, Perspectives on metabolic engineering for increased lipid contents in microalgae, *Biofuels*, 2012, **3**(1), 71–86, DOI: **10.4155/BFS.11.147**.

59 M. W. Fields, A. Hise, E. J. Lohman, *et al.*, Sources and resources: Importance of nutrients, resource allocation, and ecology in microalgal cultivation for lipid accumulation, *Appl. Microbiol. Biotechnol.*, 2014, **98**(11), 4805–4816, DOI: **10.1007/S00253-014-5694-7/FIGURES/3**.

60 M. Morales, C. Aflalo and O. Bernard, Microalgal lipids: A review of lipids potential and quantification for 95 phytoplankton species, *Biomass Bioenergy*, 2021, **150**, 106108, DOI: **10.1016/j.biombioe.2021.106108**.